Computer simulation studies of confined liquid-crystal films

Greg D. Wall and Douglas J. Cleaver
Division of Applied Physics, Materials Research Institute, Sheffield Hallam University, Pond Street, Sheffield S1 1WB, United Kingdom
(Received 20 June 1997)

In this paper we present results from molecular dynamics simulations performed using a system of Gay-Berne particles confined between two substrates in a slab geometry. We use a nonseparable anisotropic molecule-substrate interaction potential and investigate weak and moderate molecule-substrate coupling strengths. We find that for both coupling strengths a well-defined, tilted molecular layer forms at each wall and that the pretilt angle and layer density are only weakly dependent on temperature as the central region is cooled through isotropiclike and nematiclike regions. The orientationally ordered fluid formed at the center of the film is tilted in sympathy with the surface layers. At low temperatures, however, where the central region adopts a layered arrangement, a sharp change is observed in the pretilt angle. This transition is more marked in the weak-coupling system where the high-temperature tilted surface layers adopt an approximately planar arrangement at low temperatures and the system resembles a bookshelf-geometry smectic film. In the moderate-coupling system, the surface layers maintain some tilt in the presence of the layered central region, leading to a smectic-stripe phase arrangement. [S1063-651X(97)11510-0]

PACS number(s): 61.30.Gd, 61.30.Cz, 68.45.Da, 68.10.Cr

I. INTRODUCTION

Substrate-induced alignment of molecular orientations is an area of considerable interest since all liquid-crystal devices rely, at some level, on surface pinning. There has been considerable experimental interest in this area in recent years [1]. Scanning tunneling microscopy (STM) studies of the interface between a droplet of liquid-crystalline material (8CB) and a planar substrate (cleaved pyrolytic graphite) have shown that the first adsorbed layer of mesogenic molecules forms a highly ordered structure [possibly a two-dimensional (2D) crystal] stretching for thousands of angstroms [2]. In this structure, the molecules' long axes lie in a plane parallel to the substrate and form slightly interdigitated smecticlike rows. More recent temperature-dependent STM observations [3] indicate that these ordered surface structures can be disrupted or destroyed by changes in the bulk order, suggesting that bulk transitions lead to changes in surface-region order. Specifically, for the 8CB on graphite system, the 2D crystal structure of the first adsorbed monolayer is found to be destroyed at the *bulk* nematic-smectic transition temperature. Friction measurements performed on films of smectic liquid crystal also suggest a coupling between the positional ordering of the bulk and this adsorbed monolayer: they show a periodic modulation consistent with a structured adsorbed layer moving with the substrate wall [4] and regularly coupling and decoupling with the bulk smectic when sheared past it. Second harmonic generation (SHG) studies of similar systems indicate that the first adsorbed monolayer tends to be tilted with respect to the surface plane [5]. While the observation of tilted structures with SHG may be attributable to the different substrate materials used (e.g., mica rather than graphite), recent simulation results suggest that the invasive nature of the STM technique may promote planar structure [6]. SHG studies have also observed phase transitions. Specifically Jérôme *et al.* have observed a concentration-dependent anchoring transition when volatile ethylene glycol is added to 5OCB adsorbed on mica. In this case, since the ethylene glycol is preferentially adsorbed at the substrate (and is present only at weak concentrations in bulk) the transition appears to be surface driven [7].

There is a considerable body of theoretical work concerning the effects of confinement on liquid-crystalline order, much of which concerns the associated shifting and weakening of the nematic-isotropic transition [8]. More recently, Teixeira and Sluckin [9] have used Landau theory to investigate the orientational and positional order adopted at the liquid-crystal–solid interface. In this, they investigate the way in which structures in the interfacial region vary with the forms and relative strengths of the molecule-molecule and molecule-substrate interaction potentials. This work predicts that perpendicular, planar, and tilted adsorbate structures can arise from cylindrically symmetric molecular potentials at perfectly smooth substrates.

The literature contains relatively few simulation studies of liquid-crystalline systems confined in slab geometry, due largely to the considerable time scales associated with the processes involved. The lattice-based Lebwohl-Lasher model has been used to investigate the suppression of the nematic-isotropic transition [10]. This has offered a useful comparison with the early theoretical work on confined liquid crystals, but this system's simplicity (no density variation or spatial disorder is incorporated) renders it unable to model details of the interfacial structure. Specifically, the competing effects of surface packing density and orientation are not incorporated, and so there is no possibility of observing many of Teixeira and Sluckin's predicted scenarios. Enabling these requires use of an off-lattice model, such as the Gay-Berne model [11], with an appropriate particle-substrate interaction. While the bulk behavior of the Gay-Berne model is well documented [12,13], until recently only a brief investigation has been performed in slab geometry [14]. Moreover, this employed a molecule-substrate potential which was separable into its angular and spatial parts (i.e., the lo-

 © 1997 The American Physical Society

cation of the minimum in this potential was independent of the orientation of the molecule relative to the substrate). This oversimplification precluded the observation of either parallel or tilted layers arising due to competing effects at the interface.

A recent paper by Zhang *et al.* [15], which presents simulations of a confined Gay-Berne system with a *nonseparable* particle-substrate interaction potential, has confirmed Teixeira and Sluckin's predictions that suitable tuning of the molecule-surface interaction can lead to a range of different pretilt orientations. However, Ref. [15] concentrated almost exclusively on the effects of particle-substrate coupling on the surface-region structure and did not explore any temperature-dependent effects arising due to the various degrees of orientational and positional order available to the system. Subsequently, Stelzer *et al.* [16] published a very brief investigation of a similar system. This latter work employed a separable particle-substrate interaction potential and was restricted to a single state point. Furthermore, the method used to generate the starting configuration was to instantaneously impose walls on an equilibrated *bulk* nematic configuration. As described in later sections, in our studies we have found it necessary to cool confined systems very carefully from the isotropic phase in order to avoid quenching in metastable states. This experience, combined with the observation that the final configuration shown by Stelzer *et al.* exhibits regions with considerable director distortion, leads us to consider that the results presented in Ref. [16] do not correspond to the equilibrium state.

In this paper we present the results of molecular-dynamics (MD) simulations that investigate the temperature dependence of a Gay-Berne fluid confined in a slab geometry. In the next section, we present the interaction potentials used (which differ somewhat from those used previously) and list other simulation details. This is followed by a Results section and a Discussion.

II. MODEL AND SIMULATION DETAILS

Throughout we have used the standard Gay-Berne [11] potential for the particle-particle interactions. Thus each pair of particles ij (orientations $\hat{\mathbf{u}}_i$, $\hat{\mathbf{u}}_j$, interparticle vector $\mathbf{r}_{ij} = r_{ij}\hat{\mathbf{r}}_{ij}$) interacts with a potential

$$U_{P-P}(\hat{\mathbf{u}}_i,\hat{\mathbf{u}}_j,\hat{\mathbf{r}}_{ij}) = 4\epsilon_{P-P}(\hat{\mathbf{u}}_i,\hat{\mathbf{u}}_j,\hat{\mathbf{r}}_{ij}) \times\left[\left(\frac{\sigma_0}{r_{ij}+\sigma_0-\sigma_{P-P}(\hat{\mathbf{u}}_i,\hat{\mathbf{u}}_j,\hat{\mathbf{r}}_{ij})}\right)^{12} -\left(\frac{\sigma_0}{(r_{ij}+\sigma_0-\sigma_{P-P}(\hat{\mathbf{u}}_i,\hat{\mathbf{u}}_j,\hat{\mathbf{r}}_{ij})}\right)^{6}\right], \tag{1}$$

where the shape parameter $\sigma_{P-P}(\hat{\mathbf{u}}_i,\hat{\mathbf{u}}_j,\hat{\mathbf{r}}_{ij})$ is given by

$$\sigma_{P-P}(\hat{\mathbf{u}}_i,\hat{\mathbf{u}}_j,\hat{\mathbf{r}}_{ij}) = \sigma_0\left[1-\frac{1}{2}\chi\left\{\frac{(\hat{\mathbf{r}}_{ij}\cdot\hat{\mathbf{u}}_i+\hat{\mathbf{r}}_{ij}\cdot\hat{\mathbf{u}}_j)^2}{1+\chi(\hat{\mathbf{u}}_i\cdot\hat{\mathbf{u}}_j)} + \frac{(\hat{\mathbf{r}}_{ij}\cdot\hat{\mathbf{u}}_i-\hat{\mathbf{r}}_{ij}\cdot\hat{\mathbf{u}}_j)^2}{1-\chi(\hat{\mathbf{u}}_i\cdot\hat{\mathbf{u}}_j)}\right\}\right]^{-1/2} \tag{2}$$

and the well depth anisotropy is given by

$$\epsilon_{P-P}(\hat{\mathbf{u}}_i,\hat{\mathbf{u}}_j,\hat{\mathbf{r}}_{ij}) = \epsilon_0\epsilon_1^{\nu}(\hat{\mathbf{u}}_i,\hat{\mathbf{u}}_j)\epsilon_2^{\mu}(\hat{\mathbf{u}}_i,\hat{\mathbf{u}}_j,\hat{\mathbf{r}}_{ij}), \tag{3}$$

with

$$\epsilon_1(\hat{\mathbf{u}}_i,\hat{\mathbf{u}}_j) = [1-\chi^2(\hat{\mathbf{u}}_i\cdot\hat{\mathbf{u}}_j)^2)]^{-1/2} \tag{4}$$

and

$$\epsilon_2(\hat{\mathbf{u}}_i,\hat{\mathbf{u}}_j,\hat{\mathbf{r}}_{ij}) = 1-\frac{1}{2}\chi'\left\{\frac{(\hat{\mathbf{r}}_{ij}\cdot\hat{\mathbf{u}}_i+\hat{\mathbf{r}}_{ij}\cdot\hat{\mathbf{u}}_j)^2}{1+\chi'(\hat{\mathbf{u}}_i\cdot\hat{\mathbf{u}}_j)} + \frac{(\hat{\mathbf{r}}_{ij}\cdot\hat{\mathbf{u}}_i-\hat{\mathbf{r}}_{ij}\cdot\hat{\mathbf{u}}_j)^2}{1-\chi'(\hat{\mathbf{u}}_i\cdot\hat{\mathbf{u}}_j)}\right\}. \tag{5}$$

The parameter χ is determined by the length to breadth ratio σ_s/σ_e via

$$\chi = \frac{(\sigma_s/\sigma_e)^2-1}{(\sigma_s/\sigma_e)^2+1} \tag{6}$$

while χ' is related to the associated well depth ratio ϵ_s/ϵ_e, through

$$\chi' = \frac{(\epsilon_s/\epsilon_e)^{1/\mu}-1}{(\epsilon_s/\epsilon_e)^{1/\mu}+1}. \tag{7}$$

The results presented herein were all obtained using a parametrization of this model which has been well characterized for 3D bulk systems by De Miguel *et al.* [13], that is, $\sigma_s/\epsilon_e=3$, $\epsilon_s/\epsilon_e=5$, $\mu=2$, $\nu=1$. No potential cutoffs have been employed.

In the same spirit as that adopted by Gay and Berne in their choice of the Lennard-Jones-like form of Eq. (1), we have used a substrate-particle interaction based on the integrated Lennard-Jones form adopted in studies of adsorption of simple liquids. Integration of the Lennard-Jones potential over the half space beyond the substrate plane z_0 gives the substrate-atom potential

$$U_{S\text{-atom}}(|z_i-z_0|) = 4\epsilon\left[\frac{\pi}{6}\left(\frac{\sigma}{|z_i-z_0|}\right)^9-\frac{\pi}{45}\left(\frac{\sigma}{|z_i-z_0|}\right)^3\right]. \tag{8}$$

The equivalent half-space integral for the Gay-Berne particle Lennard-Jones site interaction requires numerical techniques and so represents an unacceptably high computational load for the current simulation study. As a simpler alternative, we have employed the particle substrate potential

$$U_{S-P}(\theta_i,|z_i-z_0|) = \alpha\epsilon_{S-P}(\theta_i)\left(\frac{9}{10(1-\chi^2)^{\nu}}\right)^{1/2} \times\left[\frac{2}{15}\left(\frac{\sigma_0}{|z_i-z_0|+\sigma_0-\sigma_{S-P}(\theta_i)}\right)^9 -\left(\frac{\sigma_0}{|z_i-z_0|+\sigma_0-\sigma_{S-P}(\theta_i)}\right)^3\right], \tag{9}$$

where $\cos(\theta_i)=u_{z,i}$, the shape parameter is a straightforward generalization of that used for the Gay-Berne particle Lennard-Jones site interaction

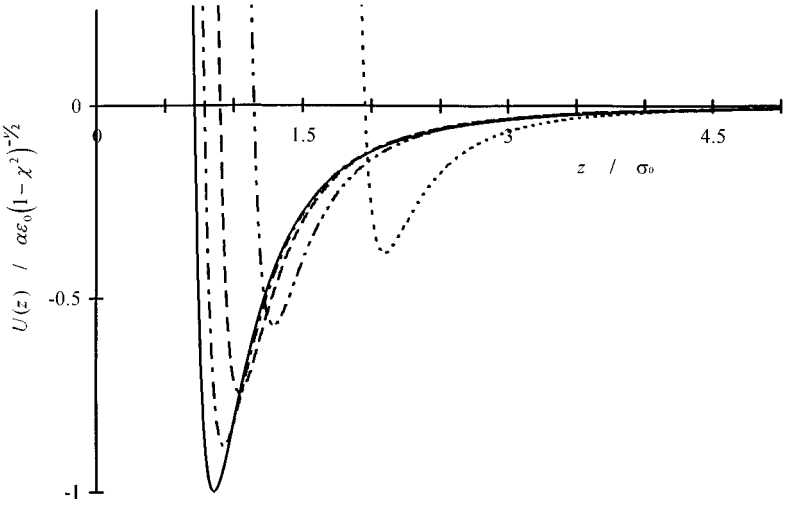

FIG. 1. Particle-substrate interaction potential $U_{S\text{-}P}(\theta,z)$ as a function of separation z, for a range of particle orientations: $\cos(\theta)=0.0$ (solid line); $\cos(\theta)=0.4$ (dash-dotted line); $\cos(\theta)=0.6$ (dashed line); $\cos(\theta)=0.8$ (dash-dot-dotted line); $\cos(\theta)=1.0$ (dotted line).

$$\sigma_0\text{-}\sigma_{S-P}(\theta_i)=\sigma_0\left[1-\left\{\frac{1}{1-\chi\,\cos^2(\theta_i)}\right\}^{1/2}\right], \qquad (10)$$

and the well depth anisotropy similarly becomes

$$\epsilon_{S\text{-}P}(\theta_i)=\epsilon_0[1-\chi'\cos^2(\theta_i)]^{\mu}. \qquad (11)$$

The one new parameter we have introduced is the scalar α, which governs the relative strengths of particle-particle and substrate-particle interactions. Specifically, the maximum well depth in the substrate-particle potential for a molecule oriented parallel to a surface is a factor of α greater than that of the Gay-Berne (GB) potential for two particles in side by side, parallel alignment. We illustrate this nonseparable substrate-particle interaction potential (9) in Fig. 1. We note that this aims to represent the interaction between an anisotropic molecule and a smooth substrate with no internal structure. Thus the increase in well depth with decrease in $\cos(\theta_i)$ should be viewed as being due to the increased molecule-substrate contact rather than to preferential alignment due to any other process. The substrate-particle interaction used by Zhang *et al.* [15] in their simulations of a confined Gay-Berne fluid was also of the ''9-3'' type, specifically

$$U_{S\text{-}P}^{\text{Zhang}}(\theta_i,|z_i-z_0|)=4\alpha\epsilon_{S\text{-}P}(\theta_i)\left[\left(\frac{\sigma_{S\text{-}P}(\theta_i)}{|z_i-z_0|}\right)^9-\left(\frac{\sigma_{S\text{-}P}(\theta_i)}{|z_i-z_0|}\right)^3\right]. \qquad (12)$$

We have adopted the more complicated shifted form of Eq. (9) since, as shown by Gay and Berne [11], this alleviates the unrealistic feature that the *width* of the potential well is strongly dependent on the molecular orientation. We also note that, while Zhang *et al.* suggest adding an extra term to Eq. (12) to break azimuthal symmetry and so model the effects of rubbed polymer substrates, the same effect may be modeled using lower symmetry shape parameter and well depth anisotropy terms in Eq. (9).

Our simulations have all been performed using standard MD techniques on a system of 256 particles in the constant NVT ensemble. Periodic boundary conditions were imposed in the x and y directions, the two substrates being normal to the z axis and separated by $13\sigma_0$. Except where explicitly stated, in what follows we have employed a system of reduced units in which the particle mass σ_0 and ϵ_0 are set to unity. The moment of inertia orthogonal to the particle long axis was also set to 1, and the reduced time step used was 0.0015. All simulations were performed at a number density of 0.3, the x and y dimensions of the simulation box being equal. No cutoff was used for the substrate-particle interaction so that each Gay-Berne particle experienced two such interactions throughout each simulation. We report results for cooling runs for substrate-particle coupling strengths $\alpha=\sqrt{10(1-\chi^2)^{\nu}/9}\simeq 0.63$ and $4\sqrt{10(1-\chi^2)^{\nu}/9}\simeq 2.53$, corresponding to weak and moderate coupling, respectively. Each cooling run has been started from a highly disordered configuration, originally obtained by melting a fcc arrangement at a very low density. Within each cooling run, each new state point has been generated from a configuration equilibrated at the previous temperature. At each data point, we have performed up to 500 000 MD time steps as equilibration, followed by 200 000 time steps for production. These run times, which are particularly long for a system of only 256 particles, were required due to the extremely slow fluctuations observed in the relative orientation of the two surface regions.

III. RESULTS

To investigate variation across the simulated slab, we have divided our system up into 100 equidistant slices to create a series of profiles. The first of these are run-averaged density profiles, $\overline{\rho(z)}$; Fig. 2 illustrates how these develop for the $\alpha=0.63$ system as the temperature is lowered. From this figure we note a well-defined surface layer at each substrate. Immediately adjacent to each surface peak is a low density trough which arises due to the excluded volume of the surface molecules. The development of $\overline{\rho(z)}$ with temperature is interpreted as follows: at high temperatures, there is virtually no structure in $\overline{\rho(z)}$ apart from the surface peaks. This is due to orientational disorder beyond the first layer, which disrupts the layering displayed by equivalent simple fluids; on cooling, $\overline{\rho(z)}$ gradually adopts the more usual

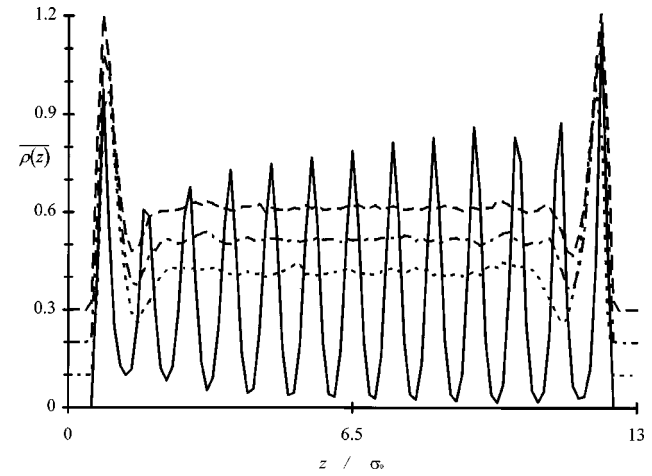

FIG. 2. Run-averaged density profiles $\overline{\rho(z)}$ for the low-coupling system at a range of temperatures: $T=0.7$ (solid line); $T=0.75$ (dotted line); $T=1.0$ (dash-dotted line); $T=1.5$ (dashed line). To aid resolution, successive curves have been shifted by 0.1 along the ρ axis.

damped oscillatory form; at very low temperatures, $\overline{\rho(z)}$ develops regular, large amplitude oscillations which traverse the whole of the slab. The heights of the surface peaks in $\overline{\rho(z)}$ increase slightly with decreasing temperature and/or increasing α, but the maxima remain at the same z values for virtually all state points investigated. The one exception to this arises at very low temperatures, where the surface peaks shift slightly towards the substrates. The $\overline{\rho(z)}$profiles for the $\alpha=2.53$ system (which we do not show here, for reasons of space) follow a trend similar to that seen at $\alpha=0.63$, except that the large amplitude oscillations are not seen at low temperatures.

The temperature dependence of the orientational order present in the system is shown in Figs. 3(a) and 3(b). For all such data, the order parameter P_2^β has been identified with the largest eigenvalue of the Q matrix,

$$Q_{AB}^{\beta}=\frac{1}{N^{\beta}}\sum_{i=1}^{N^{\beta}}\frac{3}{2}u_{A,i}u_{B,i}-\frac{1}{2}\delta_{AB}, \tag{13}$$

where δ_{AB} is the Kronecker delta, the labels $\{A,B\}$ are combinations of the axes $\{x,y,z\}$, and the superscript β (which can be ''cent'' or ''surf'') denotes the set of particles involved in the sum. For $\beta=$cent only those in the central $6.5\sigma_0$ band are used. $\beta=$surf denotes analysis performed using those particles whose orientations and locations are such that a ghost particle could not pass between them and their

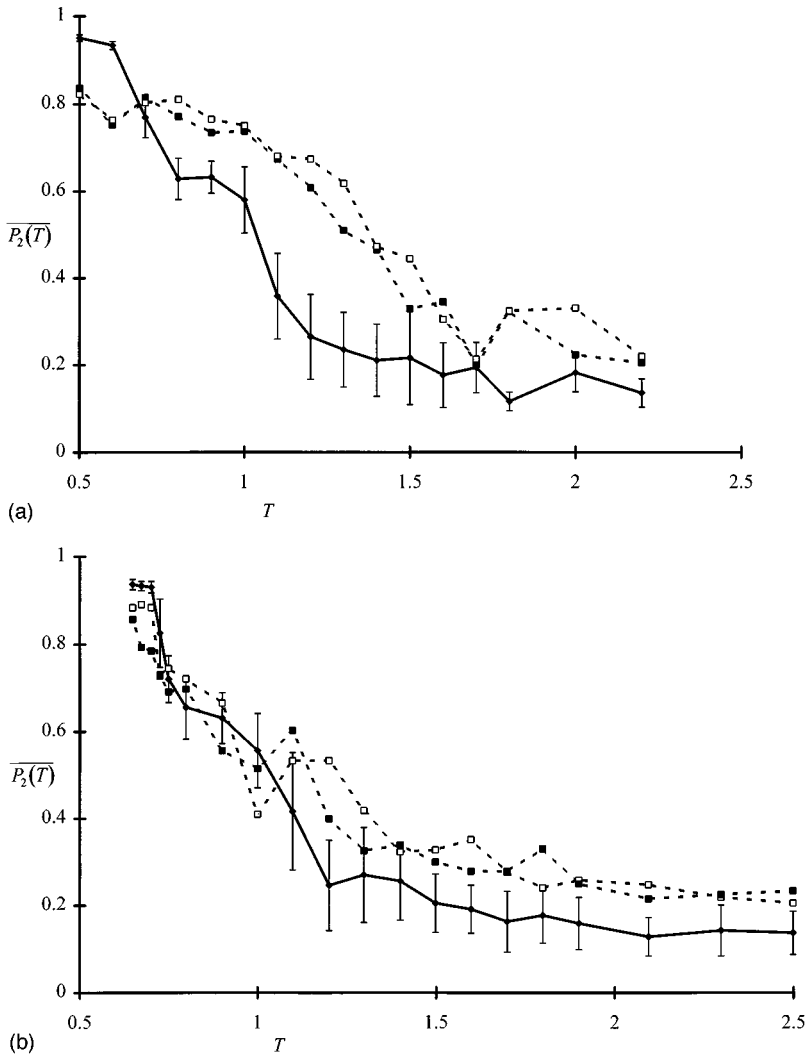

FIG. 3. Run-averaged orientational order parameters as a function of temperature for (a) $\alpha=2.53$; (b) $\alpha=0.63$. For both graphs, the key is $\overline{P_2^{\text{cent}}}\pm$one standard error (solid line); $\overline{P_2^{\text{surf}}}$ (dotted lines). The lines have no significance, and are shown simply to guide the eye.

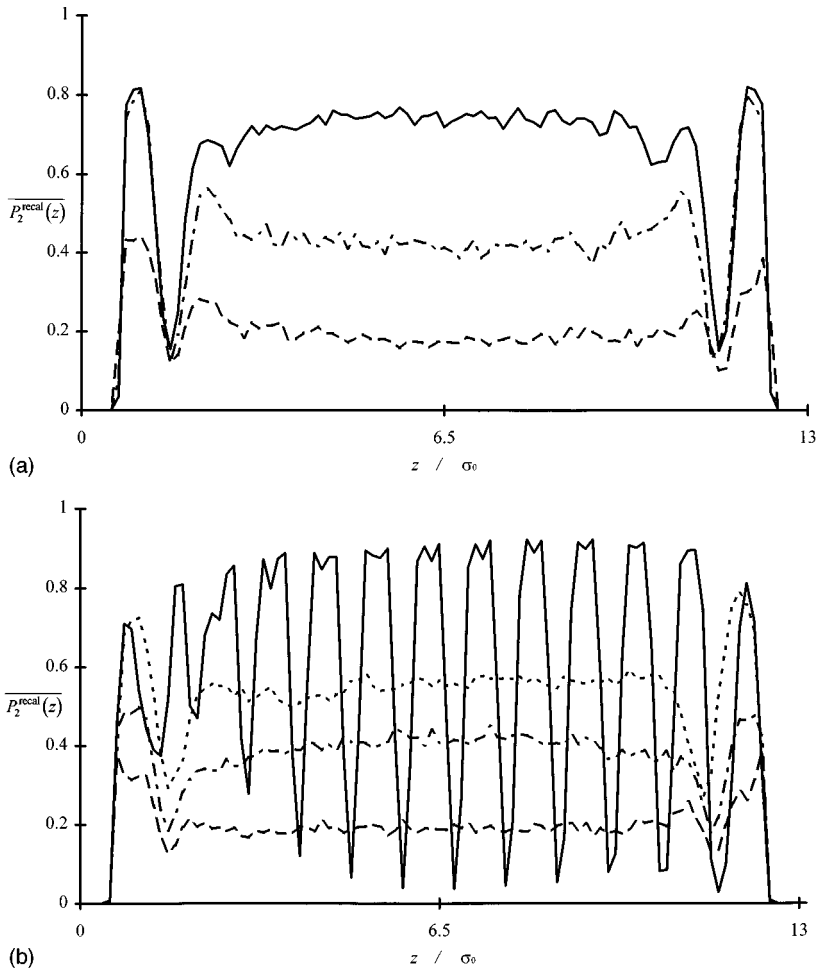

FIG. 4. Run-averaged recalibrated order-parameter profiles $\overline{P_2^{\text{recal}}(z)}$ at a range of temperatures for (a) $\alpha=2.53$; (b) $\alpha=0.63$. For both graphs, the key is $T=0.7$ (solid line); $T=0.75$ [dotted line—graph (b) only]; $T=1.0$ (dash-dotted line); $T=1.5$ (dashed line).

nearer substrate without causing a repulsive interaction. Algorithmically, the condition satisfied by such a particle is

$$|z_i-z_0|<\sigma_0+\sigma_{S-P}(\theta_i). \tag{14}$$

In compiling these data, each of the two sets of ''surf'' particles have been considered independently, so that two $\overline{P_2^{\text{surf}}}$ data sets are shown for each cooling run.

For the $\alpha=2.53$ system [Fig. 3(a)] we observe that, on cooling, the orientational order present in the central portion of the slab behaves very much like that of the 3D bulk Gay-Berne fluid: the $\overline{P_2^{\text{cent}}}$ data take the frequently seen double discontinuity form of the isotropic-nematic-smectic phase sequence. The equivalent data for the $\alpha=0.63$ system [Fig. 3(b)] displays the same behavior and are closely comparable with the $\alpha=2.53$ values. To aid description at this stage, we loosely describe the three temperature ranges suggested by these discontinuities as isotropic, nematic, and smectic; we shall subsequently return to this to characterize the observed system symmetries more fully. We note in passing, however, that the discontinuities in the $\overline{P_2^{\text{cent}}}$data are likely just to be remnants of the transitions just alluded to: these bulk transitions are known to be suppressed by substrate-induced paranematic ordering and the very narrow films being considered in this work are almost certainly below the critical thickness [8]. This view is supported by the considerable rounding of the jumps in $\overline{P_2^{\text{cent}}}$.

In both systems studied, orientational order is enhanced in the surface regions throughout the isotropic range. A small finite-size-based enhancement of this sort should be expected due to the smaller number of particles used in calculating $\overline{P_2^{\text{surf}}}$. However, this offset should decrease with increasing order, whereas for our $\alpha=2.53$ data it either remains approximately constant or increases until the smectic range is entered. For both systems studied, $\overline{P_2^{\text{surf}}}$ shows significant growth at a higher temperature than the isotropic-nematic features in $\overline{P_2^{\text{cent}}}$. As expected, $\overline{P_2^{\text{surf}}}$ is greater for $\alpha=2.53$ than for $\alpha=0.63$ for all temperatures in the nematic range. At low temperatures, $\overline{P_2^{\text{surf}}}$ saturates in the moderate coupling system, but exhibits a second discontinuity at low coupling. As a consequence, for $\alpha=2.53$ it is overtaken by $\overline{P_2^{\text{cent}}}$ when the smectic range is entered. For the $\alpha=0.63$ system, by contrast, $\overline{P_2^{\text{surf}}}$ follows $\overline{P_2^{\text{cent}}}$ closely on entering the smectic range, indicating that the highly ordered bulk is in some way enhancing the orientational order in the surface regions.

To characterize the z dependence of the orientational order, we have obtained the profile $\overline{P_2(z)}$ by implementing the Q-matrix calculation on each slice of our system. Interpretation of the resulting profile is complicated by the now substantial finite-size-based enhancement—the instantaneous occupancies of the individual slices are typically in single figures, and vary in accordance with the $\rho(z)$ profiles so that this enhancement is z dependent. In order to alleviate this difficulty, we have calculated a recalibrated order parameter

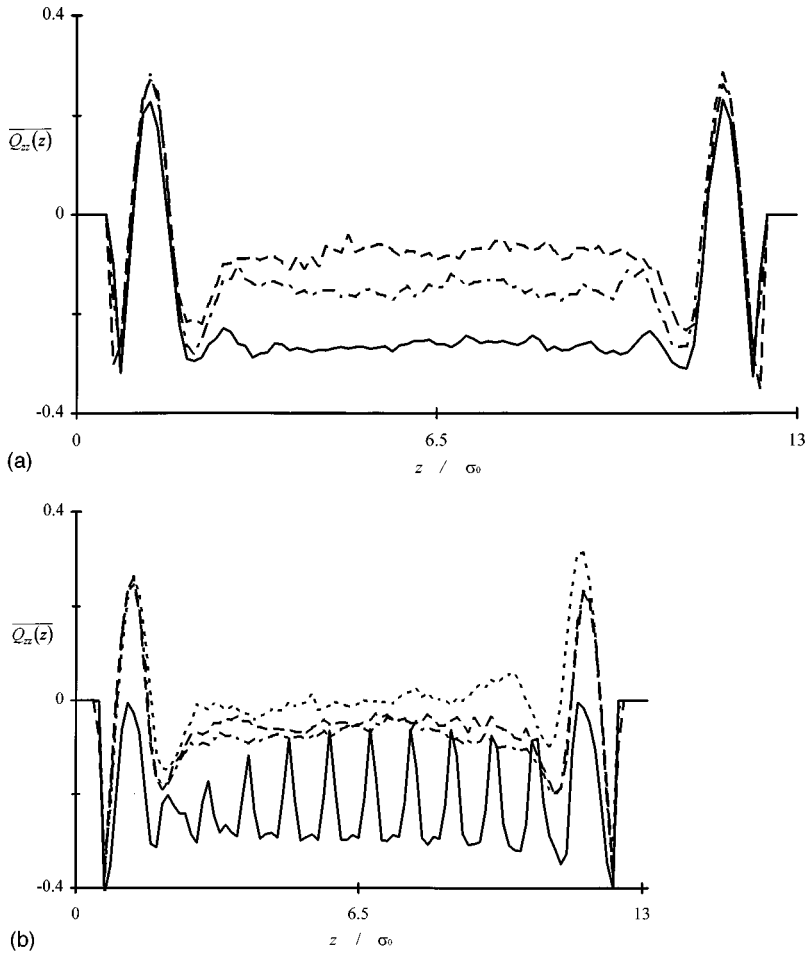

FIG. 5. Run-averaged z ordering profiles $\overline{Q_{zz}(z)}$ at a range of temperatures for (a) $\alpha=2.53$; (b) $\alpha=0.63$. For both graphs, the key is $T=0.7$ (solid line); $T=0.75$ [dotted line—graph (b) only]; $T=1.0$ (dash-dotted line); $T=1.5$ (dashed line).

$\overline{P_2^{\text{recal}}(z)}$ via a route based on Eppenga and Frenkel's expression for the order parameter in a finite system [17]. Explanation of this calculation is deferred to the Appendix.

Figure 4(a) shows typical $\overline{P_2^{\text{recal}}(z)}$ profiles obtained for the $\alpha=2.53$ system. All of these show a peak, deep trough, and a slight secondary peak associated with each liquid-substrate interface, these features being linked by a central plateau. At $T=1.0$, corresponding to the nematic temperature range, the profile is clearly u shaped, indicating that enhanced orientational order penetrates 3 to 4 σ_0 units into the film. For the lower coupling strength [Fig. 4(b)], by comparison, no secondary surface peak is apparent. Also, the $T=1.0$ profile is weakly n shaped, suggesting that in this case a slight disordering effect results from proximity to the confining substrates. This disorder would not be predicted simply by observation of the corresponding $\overline{P_2^{\text{surf}}}$ value, indicating that the low density (and low order) region which separates the bulk from the surface layer plays a significant role in determining whether a given substrate enhances or diminishes bulk order.

As well as showing this detailed structure, we note that the temperature dependences of the central plateaus and surface peaks of the $\overline{P_2^{\text{recal}}(z)}$ profiles are fully consistent with the corresponding $\overline{P_2^{\text{cent}}}$ and $\overline{P_2^{\text{surf}}}$ data. The relatively modest scatter of the values within the plateau regions indicates an acceptable level of random error in these profiles. Quantitative comparison of the plateau heights and the corresponding $\overline{P_2^{\text{cent}}}$ values indicates a consistent tendency for the former to take slightly reduced values. This systematic discrepancy is within the random error at high temperatures, but grows to about 0.1 in highly ordered films. The large amplitude oscillations in $\overline{P_2^{\text{recal}}(z)}$ for the $T=0.7$ profile match up exactly with those in the corresponding $\overline{\rho(z)}$; very low $\overline{P_2^{\text{recal}}}$ values are inevitable in low-density regions since $P_2^{\text{recal}}\equiv 0$ for any slice with an instantaneous occupancy of 1.

Two further sets of profiles are shown in Figs. 5(a) and 5(b). These depict $\overline{Q_{zz}(z)}$, the run- and density-averaged orientational order with respect to the substrate normal. All of these profiles have a sharp minimum and maximum adjacent to each substrate. In all cases, this results from the form of the particle-substrate interaction potential, which favors parallel alignment (i.e., negative Q_{zz}) at small $|z-z_0|$ and increasingly orthogonal alignment (i.e., increasing Q_{zz}) at larger $|z-z_0|$. For the moderate coupling system [Fig. 5(a)], the value of Q_{zz} at the center of the film becomes increasingly negative with decrease in temperature, dropping to about -0.25. At low coupling, by contrast, Q_{zz} remains largely independent of temperature until the smectic range is reached. At this point, Q_{zz} drops to -0.3 or less in the high-density regions. Also, the sharp maxima near the substrates rise only to 0.0, rather than the 0.3 observed under all other conditions.

As well as calculating the orientational order across the system, we have obtained a measure of the relative orientations present within the slab using subsystem directors calculated for each surface and for the central region. Taking

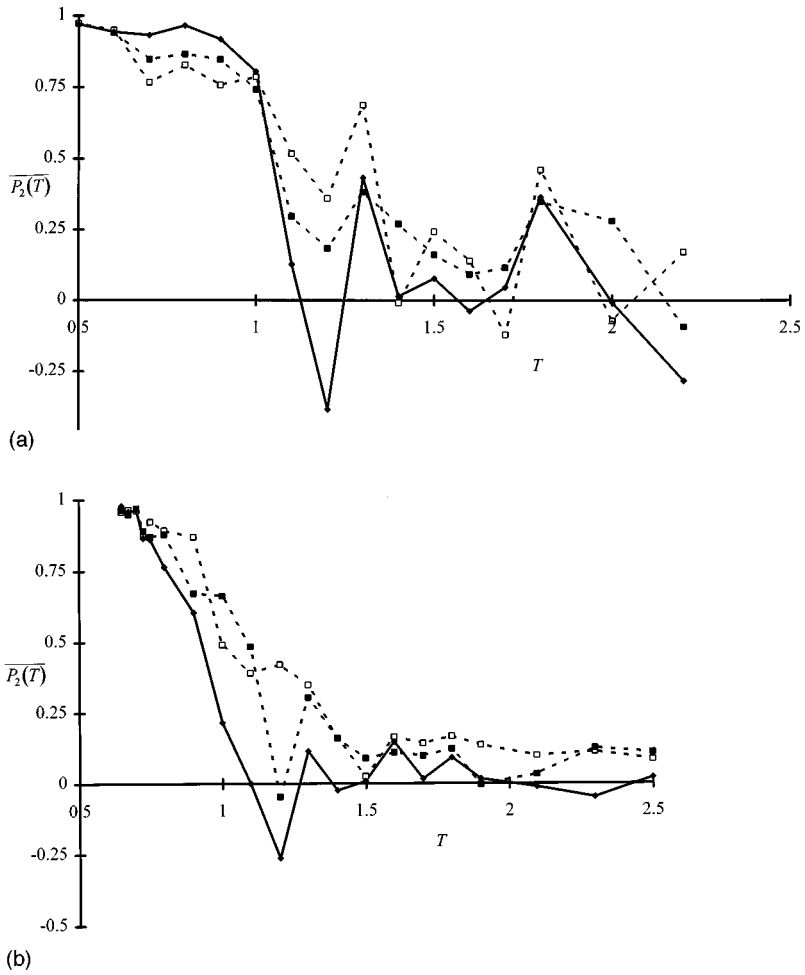

FIG. 6. Run-averaged orientational correlation order parameters as a function of temperature for (a) $\alpha=2.53$; (b) $\alpha=0.63$. For both graphs, the key is $\overline{P_2^{s\text{-}s}}$(solid line); $\overline{P_2^{s\text{-}c}}$ (dotted lines). The lines have no significance, and are shown simply to guide the eye.

the second Legendre polynomial of the dot products of the three combinations of these yields two measures of the central-region–surface-region relative orientation, $P_2^{c\text{-}s}$, and one of the relative orientation of the two surface regions $P_2^{s\text{-}s}$. Run averages of these quantities are plotted in Figs. 6(a) and 6(b). In the isotropic region, where the subsystem directors correspond to relatively disordered fluid, the measured quantities have little significance. At $T=1.2$, however, we observe that for both α values $\overline{P_2^{s\text{-}s}}$ goes negative while one of the two $\overline{P_2^{c\text{-}s}}$ becomes significantly higher than the other. This is the same temperature as that at which the two sets of $\overline{P_2^{\text{cent}}}$ data begin their isotropic-nematic rise. The asymmetry suggested by the $\overline{P_2^{c\text{-}s}}$ at this point may indicate competition between the two surface layers, as both seek to influence the preferred orientation adopted in the central region. Decreasing the temperature further brings the two surfaces into close alignment with one another and with the central region. For the $\alpha=2.53$ system, $\overline{P_2^{s\text{-}s}}$remains slightly higher than the two $\overline{P_2^{c\text{-}s}}$ values throughout the nematic range, whereas the opposite trend is seen for the $\alpha=0.63$ system. This difference is consistent with the previous observation that, within the nematic range, there is a greater orientatonal coupling between the surface layers and the central region in the $\alpha=2.53$ system. For both α values, all three measures of relative orientation converge at very high values in the smectic range.

To relate these data to the behavior within the surface layers, we have calculated a histogram of the surface-region orientational probability distribution function $\gamma(\cos\theta)$ over all particles satisfying the surface-region criterion already described. For the surface coupling of $\alpha=2.53$ [Fig. 7(a)], $\overline{\gamma(\cos\theta)}$ takes the form of a fairly wide distribution which remains centered on $\cos\theta\simeq0.65$ throughout the isotropic and nematic temperature ranges. This corresponds to an average surface molecule tilt (or pretilt) of about 40° away from the substrate normal. On entering the smectic range, $\overline{\gamma(\cos\theta)}$ exhibits a discrete shift towards a slightly more planar pretilt angle. Correlating this with Figs. 3(a) and 6(a), we conclude that for $T\leqslant1.5$ the $\alpha=2.53$ system has tilted monolayers adsorbed at each substrate. At $T\simeq1.0$ these tilted layers become highly aligned with one another. Simultaneously, the central-region fluid becomes orientationally ordered with a director reasonably close to those of the monolayers. At $T\simeq0.65$, the pretilt angle makes a small but abrupt jump at both substrates, and for the first time a *single* director applies to the entire system.

In Fig. 7(b) we show the $\overline{\gamma(\cos\theta)}$ results obtained for the surface coupling $\alpha=0.63$. Again this shows a peak centered on $\cos\theta\simeq0.65$ for virtually all temperatures, the distribution becoming slightly sharper with reducing temperature. For this lower coupling, $\overline{\gamma(\cos\theta)}$ shows a considerable change on entering the smectic temperature range; it widens and its maximum shifts to a much lower value of $\cos(\theta)$, corresponding, essentially, to a relatively disordered, planar align-

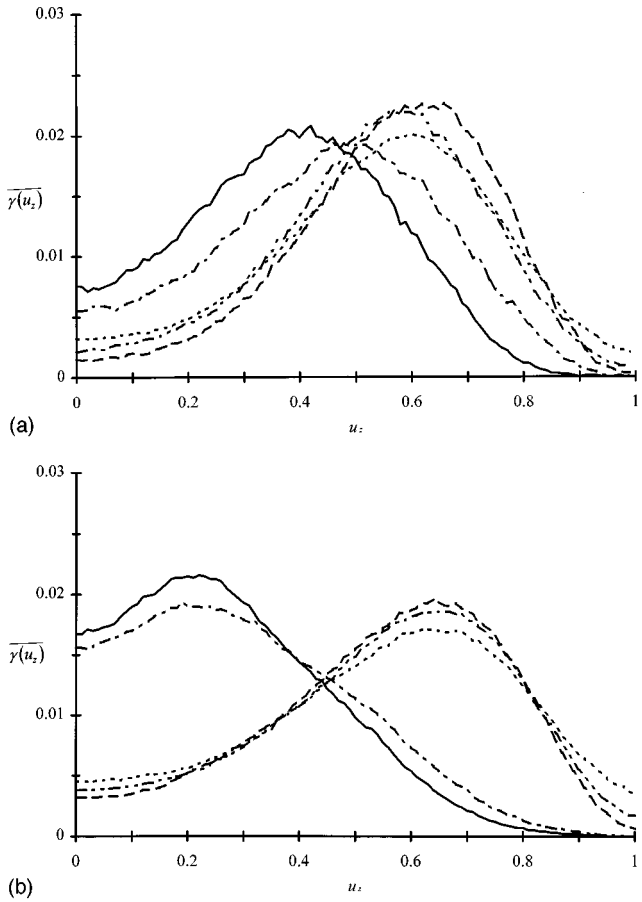

FIG. 7. Run-averaged tilt angle distribution functions of surface molecules $\gamma\ (u_z)$. (a) $\alpha=2.53$; $T=0.5$ (solid line); $T=0.6$ (dash-dotted line); $T=0.7$ (dashed line); $T=0.9$ (dash-dot-dotted line); $T=1.5$ (dotted line). (b) $\alpha=0.63$; $T=0.65$ (solid line); $T=0.7$ (dash-dotted line); $T=0.75$ (dashed line); $T=0.9$ (dash-dot-dotted line); $T=1.5$ (dotted line).

ment. This change in $\overline{\gamma(\cos\theta)}$ is consistent with the small shifts observed in the surface peaks of $\overline{\rho(z)}$ (we note, however, that no such shifts were seen by Zhang *et al.* [15] when they observed changes in the pretilt angle). In summary, the data for this lower coupling system indicate that tilted surface layers develop and, on cooling, become aligned with one another and with a tilted, orientationally ordered central region. At $T\simeq 0.7$, this system too becomes reasonably described by a single director, but this time it is planar rather than tilted.

We can confirm these interpretations by making reference to snapshots of configurations taken from the simulations. Figures 8(a)–8(c) contain typical configurations taken, respectively, from the isotropic, nematic, and smectic temperature ranges of the moderate surface coupling system. As expected, Fig. 8(a) shows a relatively disordered central region between two well-defined surface layers. Figure 8(b) shows the surface layers to be ordered and mutually aligned. They are separated by an orientationally ordered fluid whose director is tilted in sympathy with, but not perfectly parallel to, the surface layers. No positional order is apparent. By comparison, the central region of Fig. 8(c) contains well-defined planar layers, whose normal is tilted away from the substrate plane in what resembles the striped phases seen and predicted for thin smectic films [18]. While there is little evidence of the layers traversing the entire slab, there is considerable penetration of the surface layers by nonsurface molecules, a phenomenon that is not observed at all at higher temperatures. Figure 8(d) is a snapshot from the equivalent temperature range for the $\alpha=0.63$ system. Again layering is apparent at the center of the slab, but in this case the layer normal coincides with the substrate plane (i.e., a bookshelf geometry arrangement). There are some cases where these layers penetrate all the way through to the substrate, the surface molecules having attached themselves to the limbs of the central region layers. As a result, the surface layers are no longer tilted, and their centroids are shifted towards the substrates.

While Figs. 8(c) and 8(d) indicate significant positional ordering within these systems, we refrain from presenting any statistical data on this point in the present paper. The $\overline{\rho(z)}$ profile corresponding to Fig. 8(d) certainly suggests crystalline rather than smectic order. That said, there is some positional disorder apparent in the surface regions of this system, and the orientational order is not perfect. Also animations of these systems indicate some flexibility in the layers. To fully categorize the nature of these phases requires measurements of diffusion and of layer-layer positional correlations. The very small number of layers formed in this study clearly enhances the latter, however, and so renders our existing data unreliable. We shall return to this point in subsequent work based on larger systems.

IV. DISCUSSION

We have performed extensive MD simulations on a small system of Gay-Berne particles in the presence of two confining substrates at low and moderate particle-substrate coupling strengths. On cooling, both systems give clear evidence of two transitions (or remnants thereof) in the central region

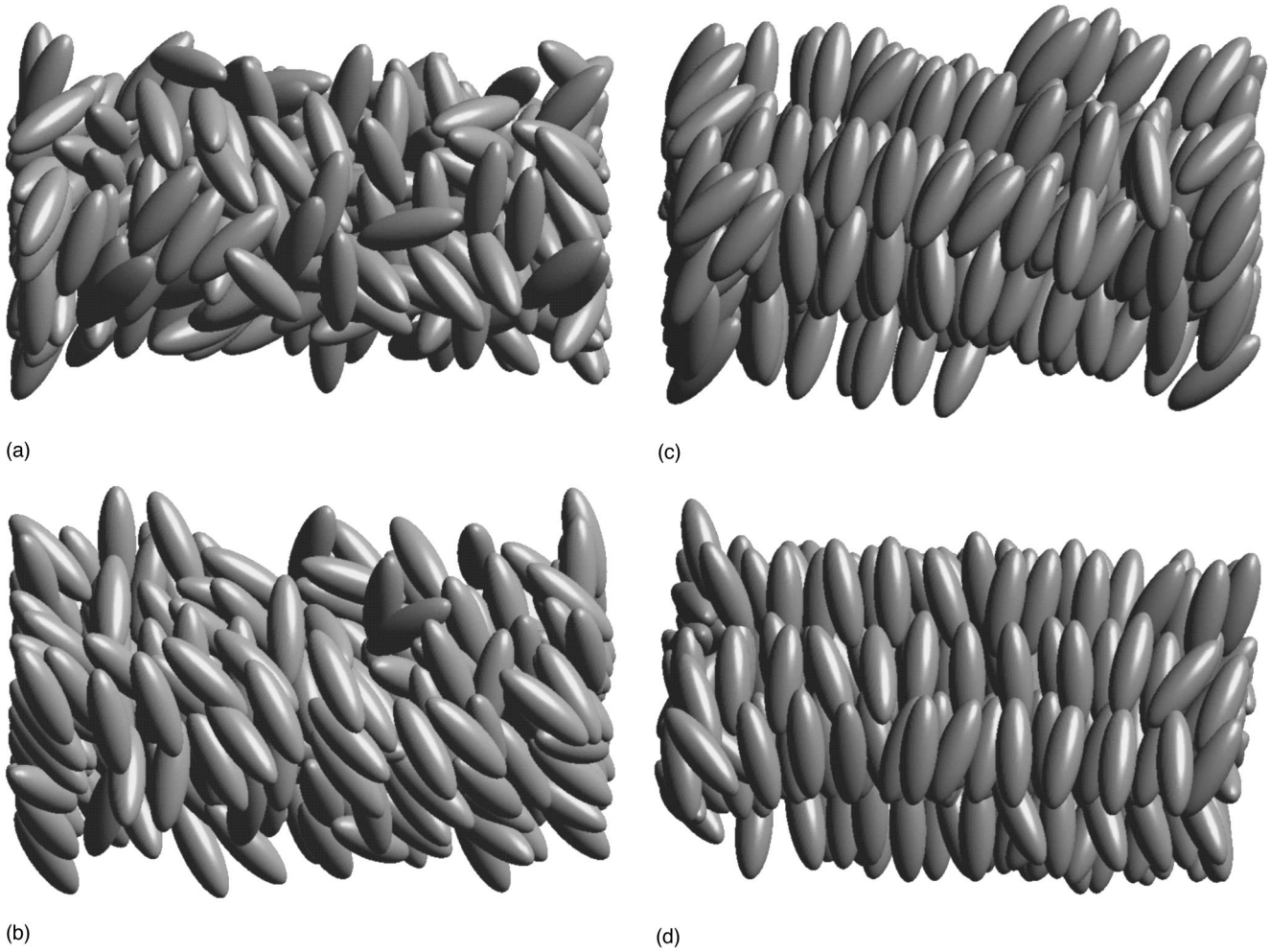

FIG. 8. Configuration snapshots for (a) $\alpha=2.53$, $T=1.5$; (b) $\alpha=2.53$, $T=1.0$; (c) $\alpha=2.53$, $T=0.7$; (d) $\alpha=0.63$, $T=0.7$.

as, respectively, orientational and positional ordering develop. For both couplings, the onset of positional order in the central region appears to induce a pretilt transition in the surface regions.

As predicted by Teixeira and Sluckin [9], and demonstrated previously by Zhang *et al.* [15], competition between packing constraints and the form of the particle-substrate interaction potential leads to the formation of a tilted layer at each substrate. Given that we have observed this despite the high symmetry of the interaction potentials employed in this work, this is clearly a general result for anisotropic particles adsorbed subject to a nonseparable potential. We note that simply increasing the strength of the particle-substrate coupling (i.e., increasing α) does *not* lead to increasingly planar layers. Rather, it results in the surface particles adopting a tighter distribution about that optimal tilt angle which maximizes the overall substrate-adsorbate interaction energy.

On cooling from high temperatures, an orientationally ordered fluid is formed in the central region of each of our confined films. This fluid is tilted with respect to the substrate normal due to the tilt of the adsorbed surface layers. Preliminary Monte Carlo simulations on these systems have shown that if cooled too rapidly, they can easily be quenched into two distinct domains of nematic order, separated by an interface which remains stable for hundreds of thousands of Monte Carlo sweeps [19]. This suggests that the central region orientational order may be seeded at the surface layers. Data presented in the preceding section show that prior to the formation of a central nematic, the surface layers have orientational order but are azimuthally uncorrelated. These same data suggest a narrow temperature range in which one surface layer's orientation becomes adopted at the center of the film; this is certainly consistent with a scenario in which the two surface regions seed domains which compete to determine the ultimate central-region director. We have found that very long run lengths are necessary in this temperature range to enable the system to develop into an orientationally ordered fluid with a reasonably uniform preferred azimuthal angle.

For the thin films studied, we have found that within the nematic temperature range, the central 50% of the system has an approximately constant order parameter. As expected, large variation in orientational order is found immediately at the surface layers. Smaller but significant variation is also found to penetrate several molecular diameters into the central fluid. This has implications for conventional continuum theory calculations (which neglect order parameter variation) of switching in confined systems, since distortions in the director field will tend to accumulate in regions of low order parameter. We note that this order parameter variation is not apparent from other measurements made and certainly could not be inferred from our density profile and surface order

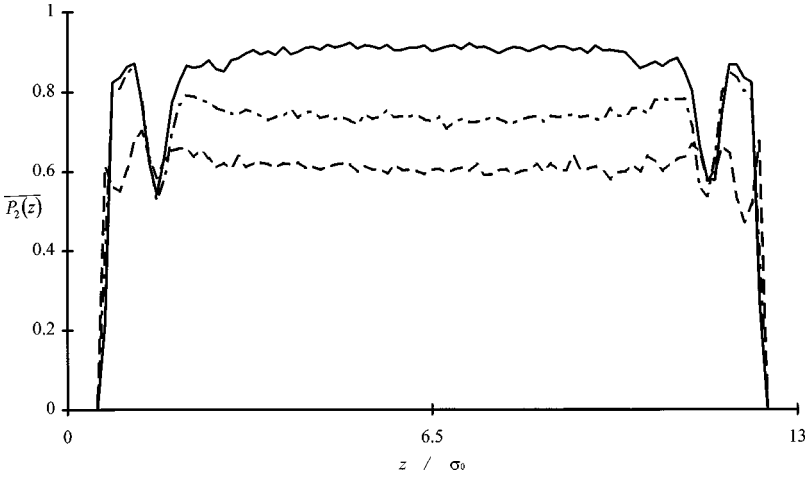

FIG. 9. Run-averaged uncalibrated order parameter profiles $\overline{P_2(z)}$ at a range of temperatures for $\alpha=2.53$; $T=0.7$ (solid line); $T=1.0$ (dash-dotted line); $T=1.5$ (dashed line).

parameter data. This is significant since, to our knowledge, existing experimental techniques are unable to determine order parameter profiles to molecular length scales: our $\overline{P_2^{\mathrm{recal}}(z)}$ profiles represent clear measurements of this effect.

While we are unable to firmly categorize the nature of the layered phases which form at the film centers at low temperatures, the effect they have on the surface layers is of considerable interest. The surface layers appear to be the major influence at the onset of orientational order in the central region, yet their role on cooling into the smectic temperature range is very passive; the changes they undergo are purely in response to the thermodynamically driven layering transition in the central region. For these two systems of common width, it is instructive to view the way in which each system resolves itself to bulk layering by considering the competition this generates between the bulk-monolayer and the monolayer-substrate interfaces. At moderate particle-substrate coupling strength, both are forced to compromise: the monolayer changes it pretilt slightly away from the optimal angle, and the tilted layers of the bulk attempt to mesh into this monolayer, despite inevitable poor packing. At low coupling, however, the now less influential monolayer-substrate interface is forced to accommodate a large change in pretilt angle, allowing the bulk-monolayer interface to virtually disappear at the limbs of the bookshelf arrangement.

The surface layers have shown two changes on cooling. At the first of these, they have become orientationally ordered, apparently without inducing any other changes in the system. In particular, the system density profile and the surface layer tilt-angle probability distribution have proved insensitive to this change. These two quantities have also been unaffected by the onset of orientational order in the film centers. Thus it is only the second change in the surface layers—the pretilt transition—that has seen modification in both their translational and orientational characteristics. This implies that the onset of bulk layering leads to the most significant change in bulk-monolayer coupling in the cooling cycle. This assertion is consistent with the friction measurements of Cagnon and Durand [4] which suggest a strong preference for registry between an adsorbed surface layer and a bulk smectic phase. We also recall the STM results of Rivera Hernandez and Miles [3], which indicate loss of positional order in the surface layer on warming through the bulk nematic-smectic transition. The implication of both these STM results and our simulations is that the pinning effect of the layered bulk phase causes the structure of the first adsorbed monolayer to change from that found at higher temperatures. Perversely, it appears that this structural change serves to *weaken* the overall interaction with the substrate.

ACKNOWLEDGMENTS

We gratefully acknowledge C. M. Care for his comments throughout this work and T. J. Sluckin and P. I. C. Teixeira for useful discussions. We are also indebted to M. J. Miles for providing us with a copy of Ref. [3] prior to its publication. This work was performed on computational hardware provided via Grant No. GR/K11956 from the UK EPSRC.

APPENDIX: CALCULATION OF RECALIBRATED ORDER PARAMETER PROFILES

It is standard procedure, when simulating liquid-crystalline systems, to identify the nematic order parameter P_2 with the largest eigenvalue, λ_+, of the Q matrix [20]. In practice, this is found to work well in ordered phases, but to give nonzero values in the isotropic phase, due to finite-size effects. In the appendix to their thin hard platelets paper [17], Eppenga and Frenkel analyzed the finite-size behavior of the three eigenvalues (λ_+, λ_0, and λ_-) of the Q matrix. In this way, they showed that in the nematic phase λ_+ provides the most accurate estimate of P_2, but that at and above the nematic-isotropic transition, the estimate based on the central eigenvalue, λ_0, coverages most rapidly with increasing system size. The relative merit of λ_0 over λ_+ in low order systems is readily apparent when one notes that since the Q matrix is traceless, λ_+ is necessarily positive for all configurations, whereas λ_0 can fluctuate about zero.

In performing their analysis, Eppenga and Frenkel derived the cubic equation

$$\lambda^3-\frac{3\lambda}{4N}[1+P_2^2(N-1)]-\frac{P_2^3}{4}-\frac{3(P_2^2-P_2^3)}{4N}-\frac{1-3P_2^2+2P_2^3}{4N^2}=0 \tag{A1}$$

linking P_2, λ, and the system particle number N. This equation was obtained by writing down the characteristic equation of the Q matrix for the general case, and averaging its

coefficients over all configurations. Inaccuracies introduced as a result of this premature averaging did not appear significant, Eq. (A1) giving good agreement with independent numerical results.

Calculating order parameter profiles across the simulation slab introduces a combination of two complications: (a) to obtain reasonable resolution across the simulation slab requires it to be divided up into very thin slices, and the instantaneous occupancies of these are inevitably very small; (b) the density profile and, hence, these occupancies are z dependent. An order parameter profile calculated by naively applying the Q-matrix technique independently to each slice of the system suffers, therefore, in that (a) there is a significant difference between the measured λ_+ values and the underlying orientational order parameters; (b) this system-size-dependent difference will be z dependent. Thus both the absolute values obtained and the qualitative z dependence observed will be distorted. Examples of profiles obtained in this way are shown in Fig. 9. As expected, these profiles suggest moderately large order parameters in the central region of the slab for all temperatures (even those for which P_2^{cent} is found to be small). Also, the values obtained show relatively little variation with either temperature or z, in contradiction with other measurements made.

In order to extract more significant information from these data, we have implemented a recalibration using Eppenga and Frenkel's expression to calculate the P_2 corresponding to each slice's instantaneous occupancy, $n(z)$, and λ_+ value. This is a straightforward operation involving solution of a cubic [or, for $n(z)=2$, a quadratic] in P_2; we denote the resulting profile $P_2^{\mathrm{recal}}(z)$. For cases where Eq. (A1) has complex solutions, we have used the alternative approximation

$$P_2^{\mathrm{recal}}(z)=P_2(z)-\langle P_2(n(z))\rangle, \tag{A2}$$

where $\langle P_2(n(z))\rangle$is the average order parameter obtained by selecting $n(z)$ orientations from a random distribution [calculating $\langle P_2(n(z))\rangle$ numerically is a trivial exercise]. These cases with complex solution arise when the instantaneous λ_+value is lower than $\langle P_2(n(z))\rangle$.

[1] B. Jérôme, Rep. Prog. Phys. **54**, 391 (1991).

[2] J. S. Foster and J. E. Frommer, Nature (London) **333**, 542 (1988); J. K. Spong, H. A. Mizes, L. J. LaComb, Jr., M. M. Dovek, J. E. Frommer, and J. S. Foster, *ibid.* **338**, 137 (1989).

[3] M. Rivera Hernandez and M. J. Miles, Scanning Microsc. (to be published).

[4] M. Cagnon and G. Durand, Phys. Rev. Lett. **70**, 2742 (1993).

[5] J. Y. Huang, R. Superfine, and Y. R. Shen, Phys. Rev. A **42**, 3660 (1990).

[6] D. J. Cleaver and D. J. Tildesley, Mol. Phys. **81**, 781 (1994); D. J. Cleaver, M. J. Callaway, T. Forester, W. Smith, and D. J. Tildesley, *ibid.* **86**, 613 (1995).

[7] B. Jérôme, J. O'Brian, Y. Ouchi, C. Stanners, and Y. R. Shen, Phys. Rev. Lett. **71**, 758 (1993); B. Jérôme and Y. R. Shen, Phys. Rev. E **48**, 4556 (1993).

[8] P. Sheng, Phys. Rev. A **26**, 1610 (1982); A. Poniewierski and T. J. Sluckin, Liq. Cryst. **2**, 281 (1987); M. M. Telo de Gama and P. Tarazona, Phys. Rev. A **41**, 1149 (1990).

[9] P. I. C. Teixeira and T. J. Sluckin, J. Chem. Phys. **97**, 1498 (1992); **97**, 1510 (1992).

[10] G. R. Luckhurst, T. J. Sluckin, and H. B. Zewdie, Mol. Phys. **59**, 657 (1986); D. J. Cleaver and M. P. Allen, *ibid.* **80**, 253 (1993).

[11] J. G. Gay and B. J. Berne, J. Chem. Phys. **64**, 3316 (1981).

[12] G. R. Luckhurst, R. A. Stephens, and R. W. Phippen, Liq. Cryst. **8**, 451 (1990); G. R. Luckhurst and P. S. J. Simmonds, Mol. Phys. **80**, 233 (1993).

[13] E. De Miguel, L. F. Rull, M. K. Challam, and K. E. Gubbins, Mol. Phys. **74**, 405 (1991).

[14] M. K. Challam, K. E. Gubbins, E. De Miguel, and L. F. Rull, Mol. Simul. **7**, 357 (1991).

[15] Z. Zhang, A. Chakrabarti, O. G. Mouritsen, and M. J. Zuckermann, Phys. Rev. E **53**, 2461 (1996).

[16] J. Stelzer, P. Galatola, G. Barbero, and L. Longa, Phys. Rev. E **55**, 477 (1997).

[17] R. Eppenga and D. Frenkel, Mol. Phys. **53**, 1303 (1984).

[18] Y. Takanishi, Y. Ouchi, H. Takezoe, and A. Fukuda, Jpn. J. Appl. Phys., Part 2 **28**, L487 (1989); L. Limat and P. Prost, Liq. Cryst. **13**, 101 (1993); S. Kralj and T. J. Sluckin, Phys. Rev. E **50**, 2940 (1994).

[19] D. J. Cleaver (unpublished).

[20] C. Zannoni, in *The Molecular Physics of Liquid Crystals,* edited by G. R. Luckhurst, and G. W. Gray (Academic, New York, 1979), pp. 191–220.